Supplemental Document

Optics EXPRESS

Manipulation of quantum dot emission with semiconductor metasurfaces exhibiting magnetic quadrupole resonances: supplement

ALEKSANDR VASKIN,[1,*] SHENG LIU,[2,3] SADHVIKAS ADDAMANE,[4] POLINA P. VABISHCHEVICH,[2] YUANMU YANG,[2] GANESH BALARISHNAN,[4] MICHAEL B. SINCLAIR,[2] THOMAS PERTSCH,[1] IGAL BRENER,[2,3] AND ISABELLE STAUDE[5]

[1] *Institute of Applied Physics, Abbe Center of Photonics, Friedrich Schiller University Jena, 07745 Jena, Germany*
[2] *Sandia National Laboratories, Albuquerque, New Mexico 87185, USA*
[3] *Center for Integrated Nanotechnologies, Sandia National Laboratories, Albuquerque, New Mexico 87185, USA*
[4] *Center for High Technology Materials (CHTM), University of New Mexico, Albuquerque, New Mexico 87131, USA*
[5] *Institute of Solid State Physics, Friedrich Schiller University Jena, 07743 Jena, Germany*
[*] *a.vaskin@tue.nl*

Supplement DOI: https://doi.org/10.6084/m9.figshare.13490241

Parent Article DOI: https://doi.org/10.1364/OE.414011

Manipulation of quantum dot emission with semiconductor metasurfaces exhibiting magnetic quadrupole resonances: supplemental document

1. METHODS

Reflectance simulations. To numerically calculate the reflectance spectra of the GaAs nanocylinder metasurfaces, we used the commercial software package COMSOL, which implements the finite element method. An elementary unit cell of the metasurface was modelled using Floquet periodic boundary conditions, an excitation port on the top, and a perfectly matched layer on the bottom. The top port acted as a source exciting a normally incident plane wave. The reflected light was detected by the same port. The silica cap and oxide pedestal were modeled with a constant refractive index of $n = 1.45$ and $n = 1.6$, correspondingly. For the optical material parameters of the GaAs we used data from Skauli et al.[1].

Photoluminescence measurements and momentum-resolved spectroscopy. A continuous wave laser emitting at 532 nm wavelength was used for the excitation. The laser was focused onto the sample by a 0.6 NA (Olympus LUCPlanFL N 40×) objective. The same objective was used to collect the emitted light in reflection, which was then propagated through a dedicated lens system to the detector. The residual laser light was filtered out by a long-pass dichroic mirror (Thorlabs DMLP650R). The lens system was adjusted to image the BFP of the collection objective onto the entrance slit (0.2 mm) of an Andor Kymera 328i spectrometer with attached iDus 1.7μm InGaAs detector and InGaAs camera (Xenics Xeva TE3). The PL spectra were measured using an iDus 1.7 μm InGaAs detector and a spectrometer grating with 150 lines per mm. The momentum-resolved spectroscopy images were taken using the same grating and Xenics Xeva TE3 as a detector. The BFP images were recorded with the same Xenics Xeva TE3 camera by opening the slit of the spectrometer and replacing the grating by a silver mirror. Bandpass filters (Thorlabs FB1150-10, FB1250-10) with center wavelengths of 1150 nm or 1250 nm and a passband width of 10 nm were placed in front of the entrance slit to selectively probe the emission in the spectral range of interest for BFP imaging.

2. MQ SCATTERING PATTERNS.

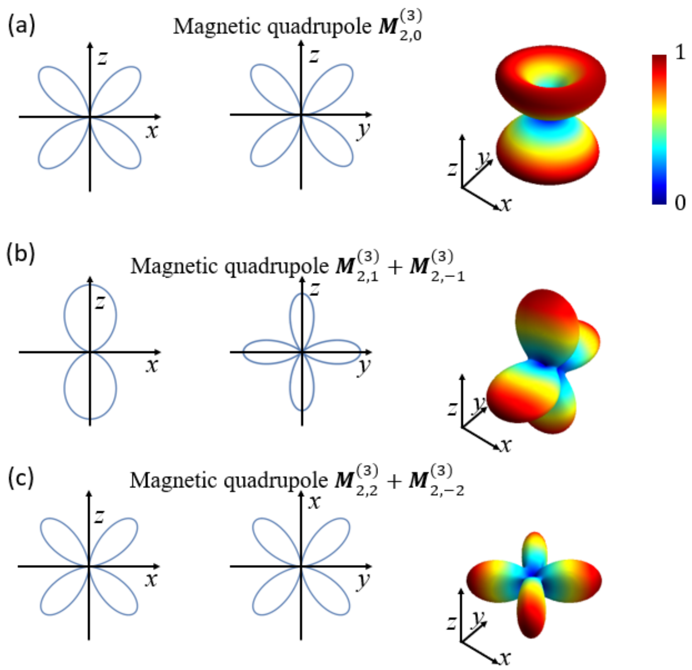

Fig. S1. Angular radiation patters of the MQ modes with different m-number. (a) $m = 0$. (b) $m = \pm 1$. (c) $m = \pm 2$.

3. TILTED NANOCYLINDERS.

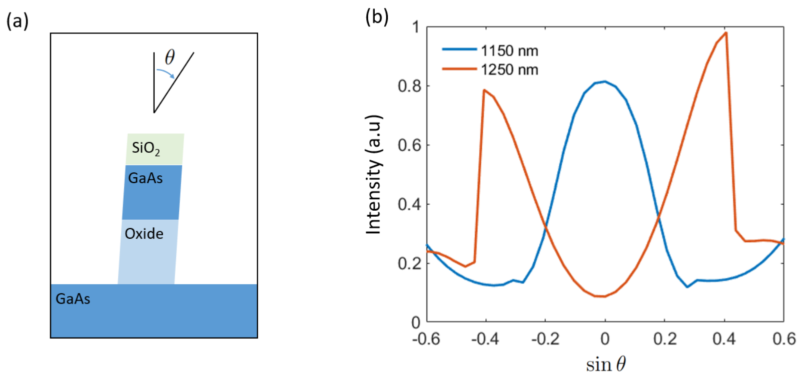

Fig. S2. (a) Illustration of the unit cell used in calculations. The axis of the nanocylinder is tilted by 2°. (b) Calculated cross-section of the BFP image at 1150 nm and 1250 nm wavelength for the metasurface consisting of tilted nanocylinedr.

To confirm that the asymmetry in the experimental BFP images is caused by the sample imperfections, we simulated a metasurface composed of nanocylinders that are tilted by 2° [2]. Since the computational domain can no longer be effectively divided into layers that are uniform along the z-axis, as needed for efficient FMM calculations, we used the COMSOL package in combination with the reciprocity principle for these simulations. S3 (a) shows a sketch of the unit cell used in our simulations. The axis of the cylinder was tilted by $\theta = 2°$. A TE or TM plane wave was incident from the air semi-space onto the metasurface. The polar angle of incidence θ was varied from 0° to 37° corresponding to the NA of the collection optics and the azimuthal angle of incidence ϕ was fixed to 0°. Therefore, the wavevector of the incident plane wave stays in the plane of the S3 (a). S3 (b) shows the calculated intensity distribution over the vertical cross-section through the center of BFP images at 1150 nm and 1250 nm wavelength (see Fig. 4 in the main text). We observe a pronounced asymmetry of the BFP image of $m = \pm 1$ MQ mode at 1250 nm, while the $m = \pm 1$ MQ mode at 1150 nm appears fairly symmetric as in the experiment.

4. EMISSION CALCULATIONS FOR NA=1.

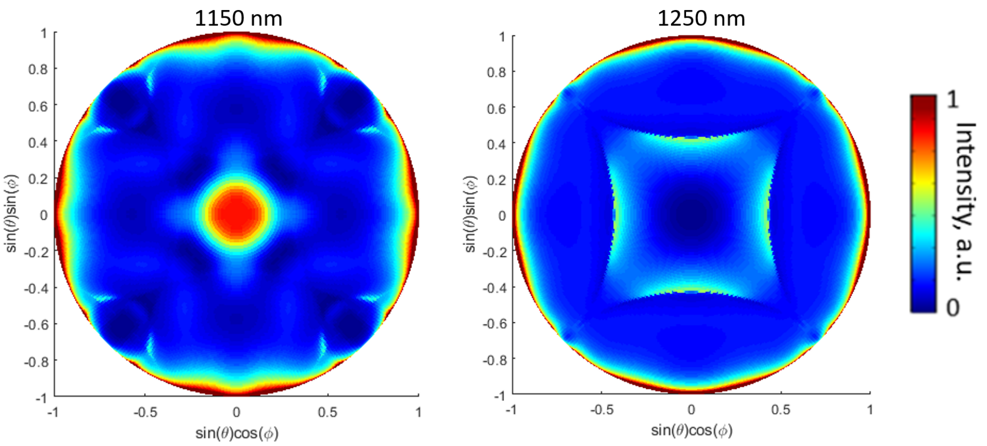

Fig. S3. Calculated BFP images at 1150 nm and 1250 nm wavelength for NA=1.

REFERENCES

1. T. Skauli, P. S. Kuo, K. L. Vodopyanov, T. J. Pinguet, O. Levi, L. A. Eyres, J. S. Harris, M. M. Fejer, B. Gerard, L. Becouarn, and E. Lallier, “Improved dispersion relations for GaAs and applications to nonlinear optics,” J. Appl. Phys. **94**, 6447–6455 (2003).
2. F. J. F. Löchner, A. N. Fedotova, S. Liu, G. A. Keeler, G. M. Peake, S. Saravi, M. R. Shcherbakov, S. Burger, A. A. Fedyanin, I. Brener, T. Pertsch, F. Setzpfandt, and I. Staude, “Polarization-dependent second harmonic diffraction from resonant GaAs metasurfaces,” ACS Photonics **5**, 1786–1793 (2018).